Journal of Nuclear Materials 386–388 (2009) 1102–1106

Contents lists available at ScienceDirect

Journal of Nuclear Materials

journal homepage: www.elsevier.com/locate/jnucmat

Control of molten salt corrosion of fusion structural materials by metallic beryllium

P. Calderoni [a,*], P. Sharpe [a], H. Nishimura [b], T. Terai [c]

[a] Fusion Safety Program, Idaho National Laboratory, Idaho Falls, ID, USA
[b] Nuclear Professional School, Graduate School of Engineering, The University of Tokyo, Tokyo, Japan
[c] Department of Nuclear Engineering and Management, Graduate School of Engineering, The University of Tokyo, Tokyo, Japan

A B S T R A C T

A series of tests have been performed between 2001 and 2006 at the Safety and Tritium Applied Research facility of the Idaho National Laboratory to demonstrate chemical compatibility between the molten salt flibe ($2LiF + BeF_2$ in moles) and fusion structural materials once suitable fluoride potential control methods are established. The tests adopted metallic beryllium contact as main fluoride potential control, and the results have been published in recent years. A further step was to expose two specimens of low activation ferritic/martensitic steel 9Cr–2W to static corrosion tests that include an active corrosion agent (hydrofluoric gas) in controlled conditions at 530 °C, and the results of the tests are presented in this paper. The results confirmed the expected correlation of the HF recovery with the concentration of metallic impurities dissolved in the salt because of specimen corrosion. The metals concentration dropped to levels close to the detectable limit when the beryllium rod was inserted and increased once the content of excess beryllium in the system had been consumed by HF reduction and specimen corrosion progressed. Metallographic analysis of the samples after 500 h exposure in reactive conditions showed evidence of the formation of unstable chromium oxide layers on the specimen's surface.

1. Introduction

In 2001, the Fusion Safety Program of the Idaho National Laboratory started a research program as a part of the 2nd Japan/US Program on Irradiation Tests for Fusion Energy Research (JUPITER-II) aimed at the characterization of the molten salt flibe ($2LiF + BeF_2$ in moles) as a breeder and coolant material for fusion applications [1]. The program focused on the two most important technological challenges related to molten salt breeder systems, corrosion of structural material and tritium permeation. For fluoride-based molten salts such as flibe compatibility with structural materials is determined by its 'redox condition,' quantitatively defined as the chemical potential of fluoride [2,3]. Flibe redox condition is in turn affected by the radiation environment and nuclear transmutation reactions, by reactivity with other contacting materials and the gaseous environment over the salt and by interaction with impurities. The corrosive properties of fluoride molten salts were analyzed during the operation of the Molten Salt Reactor Experiment at the Oak Ridge National Laboratory in the 1970's [4–6]. Contrary to this fission experiment, however, in fusion systems transmutations due to neutron capture reactions constitute an inherent source of tritium and fluoride atoms within the molten salt that constantly modifies the fluoride potential. The dominant transmutation reactions of flibe constituents (using standard neutron reaction theory nomenclature) are relative to its tritium breeder element (lithium),

$$\begin{aligned} &^6\mathrm{Li}(n,\alpha)^3\mathrm{H}, \\ &^7\mathrm{Li}(n,n'\alpha)^3\mathrm{H}, \end{aligned} \tag{1}$$

and its neutron multiplier element (beryllium),

$$\begin{aligned} &^9\mathrm{Be}(n,2n)2^4\mathrm{He}, \\ &^9\mathrm{Be}(n,\alpha)^6\mathrm{He}(T_{1/2}=807\ \mathrm{ms}) \rightarrow {}^6\mathrm{Li}. \end{aligned} \tag{2}$$

The overall result of the above nuclear reactions (aside from the main purpose of generating tritium) is the production of free fluoride that had been associated with the transformed cations. The fluoride ions can either combine with the tritium produced to form tritium fluoride (TF), combine with other metal impurities in the flibe, or remain as fluoride ions. Experimental studies of flibe irradiation in fission reactors with a fast neutron spectra have shown that without active chemical control more than 90% of the tritium generated in the molten salt accumulates as tritium fluoride [7–10] and recent estimates based on typical blanket parameters have quantified its generation as ranging from $1.2e^{18}$ to $1.33e^{18}$ atoms TF per m^3 per s [11]. This would lead to unacceptable corrosion rates of all metallic structural materials presently considered because of the strong chemical reactivity of tritium fluoride that combine with metallic elements following the general reaction:

$$2^3\mathrm{HF} + \mathrm{M} \leftrightarrow \mathrm{H}_2 + \mathrm{MF}_2, \tag{3}$$

* Corresponding author. Tel.: +1 208 533 4547; fax: +1 208 533 4207.
E-mail address: Pattrick.Calderoni@inl.gov (P. Calderoni).

0022-3115/$ - see front matter © 2009 Elsevier B.V. All rights reserved.
doi:10.1016/j.jnucmat.2008.12.292

(where ^3H could be any other hydrogen isotope and M could be Fe, Cr, W, etc. depending on the specific structural material considered), therefore the design of an active control of the fluoride potential is a key feasibility issue for molten salt blankets. Several methods are available in principle for redox control, and they can be summarized as ternary salt mixtures, cover gas control or contacting with a salt element in metallic form [3,4,12]. Methods based on ternary (or higher order) salts have been investigated for fission applications since the mixture inherently contains uranium salts as fuel, but their complexity makes them an inefficient choice for fusion applications. Gas contacting methods based on HF/H_2 mixtures are used during salt preparation, but the presence of hydrogen in the cover gas would aggravate the issue of tritium permeation making it unfeasible for fusion blankets. Thus contacting with metallic beryllium has been selected as the method of choice and investigated during the JUPITER-II Program in the redox test experimental campaign. The objective of the tests was the quantitative measurement of the rate of the Be–TF redox reaction with the goal of obtaining useful kinetic data that could be used to quantitatively validate the method [1,13–15]. To simulate tritium fluoride generation by neutron capture, hydrogen fluoride gas concentrations between 900 and 1800 ppm were provided in the gas phase by bubbling gas mixtures of HF/H_2 in excess of He in the salt. The gas phase concentration range corresponds to dissolved HF concentrations in flibe that are about 100–200 times higher than expected in a fusion blanket [1]. This limitation was imposed by the sensitivity of the instrument used to monitor the variation of the HF concentration in the gas stream. To conclude the feasibility study two specimens of low activation ferritic/martensitic steel 9Cr–2W have been exposed to static corrosion tests with the same conditions encountered in previous redox test.

2. Experimental facility and test procedures

The corrosion tests described in this paper used the same facility and similar experimental procedures of the redox tests [1]. The molten salt material was also the same used for previous experiments. It had been produced from 540 g of stoichiometrically balanced powder mixture of BeF_2 and LiF melted in a Ni crucible and purified by hydro-fluorination. Process chemistry during purification and testing was controlled by mass spectrometry along with periodic sampling and analysis by inductively coupled plasma atomic emission spectroscopy (ICP-AES) or inductively coupled plasma mass spectroscopy (ICP-MS) analysis for metallic impurities, LECO analysis (inert gas thermal evolution) for oxygen and nitrogen, and surface analysis (SEM, EDX) for reaction with contacting surfaces.

The corrosion test cell schematic is shown in Fig. 1. The outer shell bottom side (the pot) was a standard CF vacuum flange to which a mating tube with 0.15 m length and 0.1 m outer diameter had been welded. The top side (the lid) was also a standard CF blank flange on which various sized risers with CF flanges have been welded to provide gas tight access to the cell volume. Components were made of 316 stainless steel and all inner surfaces were nickel coated using a high-velocity oxyfuel spray process to reduce the surfaces reactivity with HF gas. The risers allowed the penetration of sliding tubes that housed the beryllium rod, the steel specimens and the sampling cups (Fig. 2). The sliding tubes were provided with a gas inlet to minimize air leaks and molten salt vapor condensation on the tubes inner surfaces. Two gate valves on each riser were used to minimize the access of air during sampling and specimen insertion. A third sliding seal was used for the gas inlet that carries the reactive mixture containing HF and H_2 and was immersed in the salt after melting about 5 mm from the crucible bottom. Three more gas connections were used as inlet

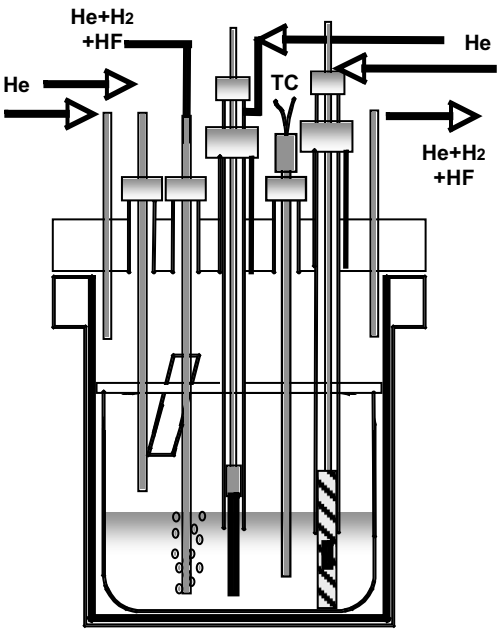

Fig. 1. Corrosion test cell schematic.

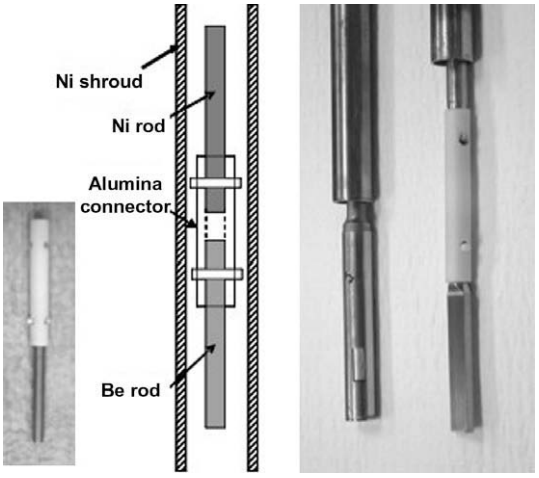

Fig. 2. From left to right: Be rod and assembly scheme, Ni sample loader, JLF-1 specimen.

for inert gas in the cell volume and above the salt surface and as outlet for all the combined input flows. The gas outlet was connected to the diagnostic system composed of a sampling quadrupole mass spectrometer (Stanford Research System SRS-100) and an on-line auto-titration system (Schott Titronic Universal) that records the volume of 0.1 N NaOH solution used to neutralize the amount of HF present in the gas stream. The measured decrease of NaOH consumption rate when metallic beryllium was contacted and then again extracted from the salt allowed the evaluation of the reaction kinetics in the system. The time period in which redox control was active is determined from the time to recover the initial NaOH consumption rate before the beryllium insertion.

The initial phase of the procedure for the two corrosion tests was derived from an optimization of previous redox tests [14]: the molten salt was first maintained at 530 °C under a bubbling He gas to establish baseline conditions, then the bubbling gas was then switched to the corrosive $He/H_2/HF$ mixture and equilibrium was re-established. The mixture chosen for the tests had a nominal total flow rate of 140 cm^3(NTP)/min with an HF concentration of

1075 ppm. The ratio of concentrations of H_2 to HF was kept at 11 as for previous redox tests. The corresponding HF molar flow rate was $1.12e^{-7}$ mol/s. At time $t = 0$ the beryllium rod (Brush Wellman I-70 high-grade beryllium) was immersed and remained in the molten salt for 5 h. Its diameter (Fig. 2) was 5.1 mm and the immersed depth estimated as 23 mm, for an estimated contact area of 387 mm^2. After 5 h the beryllium rod was extracted and the steel specimen inserted in its place to start the corrosion test, which lasted 500 h. Both specimens tested were reduced activation ferritic/martensitic steel JLF-1 (89Fe–9Cr–2 W) produced in Japan and provided by Tokyo University within the JUPITER-II collaboration. The specimens (Fig. 2) had a width of 9 mm, a thickness of 2.5 mm and the immersed height was estimated as 23 mm, for an estimated surface in contact with the salt of 552 mm^2. Based on the experience with early redox tests [14] the specimens and the beryllium rod have been electrically decoupled from the grounded nickel crucible using alumina connectors to avoid creating a low resistance path for electrochemical ionic currents in the salt between the immersed surfaces and the crucible.

3. Results and discussion

The main result of the corrosion tests was the confirmation of the expected correlation between the HF recovery used to evaluate the efficiency of metallic beryllium as a redox agent and the measured concentration of metallic impurities dissolved in the salt because of specimen corrosion. As already stated, corrosion was driven primarily by the HF contained in the gas mixture that bubbled through the salt following the general reaction expressed in (3). As the reaction proceeds the net effect is the increase of concentration of iron and other metallic elements in the salt (in the form of metal fluorides) at the expense of the structural material. Initial impurities from material processing between tests also contributed to selective Cr depletion through the reaction $MF_2 + Cr \leftrightarrow M + CrF_2$, where M could be Ni or Fe. Fig. 3 plots on the right vertical axis the main measured impurities (iron and chromium) expressed in part per million (moles) in the salt for the first 200 h of the second corrosion test (FSCT2). The titration curve relative to the same period is also plotted as the volume of 0.1 N NaOH solution expressed in milliliters (left vertical axis). The initial slope of the titration curve (time < 0) corresponded to equilibrium conditions with the mixture of $HF/H_2/He$ specified before. The beryllium rod was contacted with the molten salt at time $t = 0$, retracted after 5 h and the sample inserted in its place. The decreased consumption rate corresponds to the period of active redox control (extending about 40 h after the sample immersion). The full range (500 h) of measured chromium and iron impurities data is plotted in Fig. 4 for the first corrosion test (FSCT1), which was performed in the same conditions, and reported in Table 1 for FSCT2. Nickel impurities (reported in Table 1 for completeness) should not be compared to other elements in terms of absolute numbers because of the much larger contact area of the crucible compared to that of the specimen; tungsten impurities are usually below the detection limit of about 2 ppm in both cases and are not plotted; oxygen and nitrogen impurities are measured to evaluate process conditions. The data show that the metallic beryllium present in the system effectively controlled the fluoride potential and prevented the dissolution of metallic elements from the specimen.

It is important to note that the experiments described here were not designed to measure the effective solubility of metallic beryllium in flibe, but only to assess the feasibility of metallic beryllium as a redox agent under aggressively corrosive conditions. The presence of different materials in contact with the salt during various phases of the test (nickel crucible, beryllium rod, steel specimen, thermocouples, sampling cup) established complex electrochemical phenomena that were also responsible for excess beryllium availability in the system. For example, post-analysis inspection of nickel crucibles used during long-term beryllium contacting tests [13] showed the formation of stable Ni–Be alloys on the crucible surface. An attempt to separate the various contributions was performed by comparing the effect of electrically coupled beryllium rods versus the alumina-insulated rods showed in Fig. 2 that were also adopted for the corrosion tests [14,15]. However, conventional methods based on weight loss and post-analysis are not accurate enough when trying to measure a small quantity

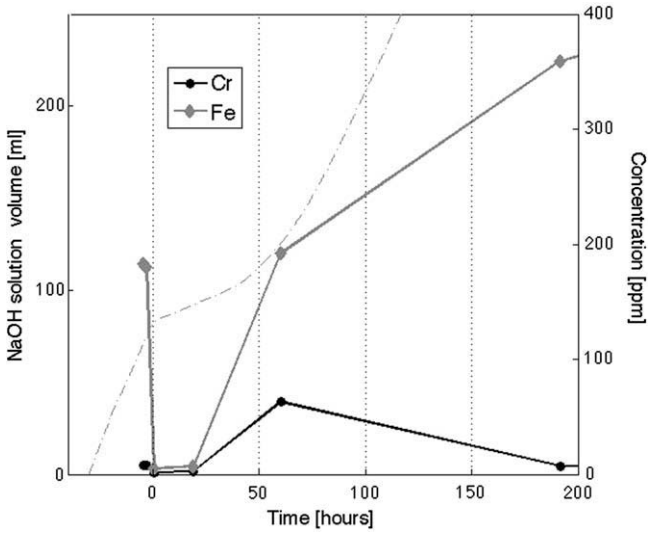

Fig. 3. Measured impurities and titration curve for FSCT2 first 200 h.

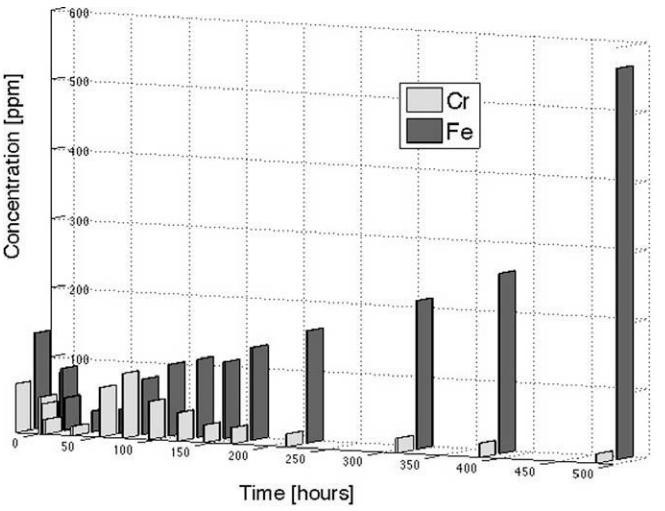

Fig. 4. Measured impurities for FSCT1.

Table 1
Flibe impurity concentrations for corrosion test sample FSCT2.

Time (h)	Fe (ppm)	Cr (ppm)	Ni (ppm)	W (ppm)	O (ppm)	N (ppm)
1	183	7.83	107	<det		
2.5	180	7.47	105	<det		
6	4.94	1.66	11	<det		
24	7.34	2.53	62.6	<det	1850	40.65
64	192	63	22.4	2.08	1890	42.25
192	359	7.24	42.2	<det	1195	24.5
336	435	9.23	74.9	<det	565	13.3
502	490	5.59	128	<det	1195	30

of an element in the presence of a large background of the same element, as is the case in measuring the solubility of excess beryllium in flibe, and ^{7}Be radioactive tracing should be employed. In terms of blanket design, the determination of the beryllium solubility would address whether a simple method based on uniform beryllium dissolution in cooling loops would be enough to balance the small TF source due to nuclear transmutations, or else localized methods for impurities control (including metallic beryllium contacting) are needed in equilibrium with acceptable corrosion rates, as is the case in sodium cooling systems.

When the titration slope was recovered the excess beryllium present in the system had been consumed and the initial, aggressively corrosive conditions were restored. As a result the concentration of measured impurities in the salt increased. The concentration of iron continued to increase during the 500 h tests, while the concentration of chromium peaked about 70 h after the test started and then decreased. The metallographic analysis of the specimens extracted from the molten salt bath offered little insight on the processes related to the redox-controlled phase because of the successive long-term exposure to highly reactive conditions. However, the results confirmed that the decrease in chromium concentration is due to the precipitation of chromium oxide layers as predicted by thermodynamic equilibrium calculations and observed in previous experiments [10]. The layers have been reported to be mainly composed of Cr_2O_3, but lower concentrations of other elements such as $(CrFe)_2O_3$, and spinel type oxides of $(FeCr_2)O_4$ and Fe_3O_4 have also been observed. Fig. 5 shows a low magnification scanning electron microscope (SEM) picture of the cross section closer to the specimen bottom tip, where the thicker layer of salt solidified during extraction is present. The formation of an oxide layer is observed in Fig. 5 as well as Fig. 6, a higher magnification SEM picture of a different cross section where successive layer formation and detachment is observed. It is clear that in the conditions of the experiments the oxide layer forming on the specimen surface is not stable. The composition of characteristic morphological structures has been quantitatively analyzed by energy dispersive X-ray spectroscopy (EDX). The results overall confirmed the presence of higher than expected oxygen concentration due to progressive deterioration of the sliding carbon seal used for sampling operations, as already observed in the LECO analysis data reported in Table 1. The EDX spectrum and elemental composition of the precipitating layer is shown in Fig. 7.

The total mass of impurities dissolved in the salt was calculated from the sampling analysis results. The data presented in Fig. 4

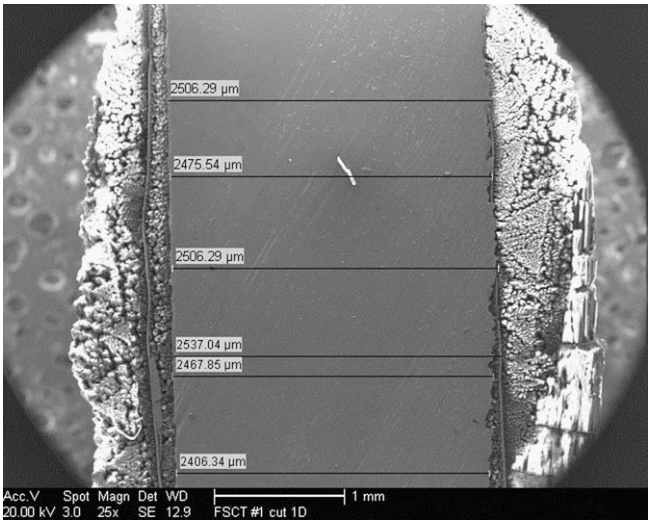

Fig. 5. Low magnification SEM picture of FSCT1 specimen.

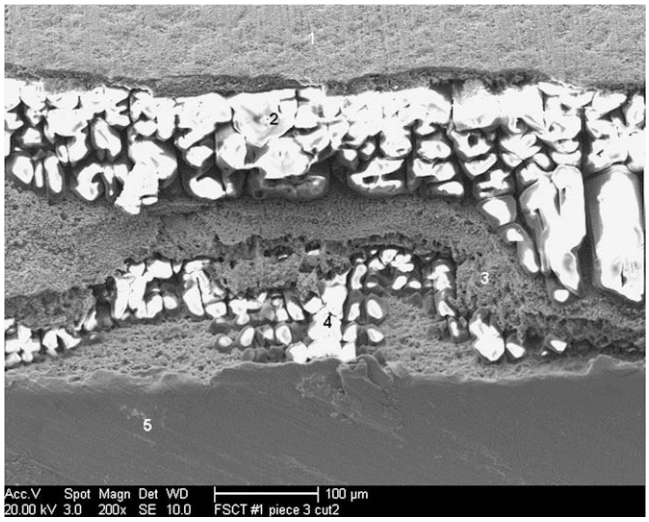

Fig. 6. Successive oxide layer formation and detachment.

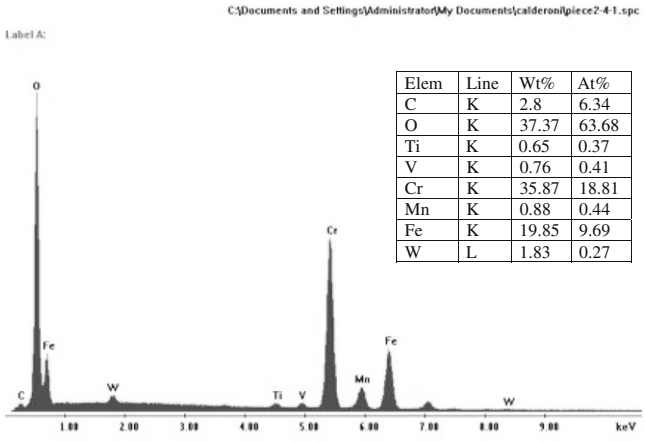

Elem	Line	Wt%	At%
C	K	2.8	6.34
O	K	37.37	63.68
Ti	K	0.65	0.37
V	K	0.76	0.41
Cr	K	35.87	18.81
Mn	K	0.88	0.44
Fe	K	19.85	9.69
W	L	1.83	0.27

Fig. 7. EDX analysis of precipitated layer.

have been interpolated and the integration of the fitted curves over the test period yielded a total mass of $8.1688e^{-2}$ g of Fe and $9.5679e^{-3}$ g of Cr. The lower ratio of Fe to Cr impurities compared to the metal composition and the higher ratio of Cr to Fe observed in the precipitated layers (Fig. 7) confirms the selective dissolution of chromium in the salt, although quantitative observations are not possible due to the high-non-uniformity typical of static cell tests. To a zero order approximation the dissolved mass would correspond to a 21 micron layer uniformly eroded from the specimen surface immersed in the salt. This calculation compares well with the localized erosion measured during SEM observation of various specimens cross sections (Fig. 3). The estimated corrosion rate is 370 microns/year, which also compares adequately well with previous observations for stainless steel [12] considering the highly aggressive conditions employed.

4. Conclusions

Two corrosion tests of representative fusion blanket structural material in the molten salt flibe were performed as a conclusion of an experimental campaign aimed at the feasibility assessment of metallic beryllium as a control agent of the fluoride potential, which in turn controls compatibility and corrosion properties.

The corrosion tests were performed in the same conditions as previously reported experiments, mainly characterized by the injection in the salt bath of an aggressive gas mixture containing 1075 ppm hydrogen fluoride. The main achievement was the experimental verification of the correlation between the rate of HF neutralization measured downstream of the reactor cell by a titration system and the concentration of impurities dissolved in the salt, measured by periodic sampling and analysis. Further qualitative insights on the chemical processes have been gained by metallographic analysis of one of the specimens that confirmed the selective corrosion of chromium and the precipitation of unstable layers of chromium oxide.

Acknowledgements

The US Department of Energy Office of Fusion Energy Sciences, and the Japan–US joint research program JUPITER-II partially supported the work under DOE Idaho Operations Contract DE-AC07-99ID13727.

References

[1] D.A. Petti et al., Fusion Eng. Des. 81 (2006) 1439.
[2] B.R. Sundheim, Fused Salts, McGraw Hill, 1964.
[3] D. Olander, J. Nucl. Mater. 300 (2002) 270.
[4] C.F. Baes, J. Nucl. Mater. 51 (1974) 149.
[5] S. Cantor, W.R. Grimes, Nucl. Tech. 22 (1974) 120.
[6] P.N. Haubenreich, J.R. Engel, Nucl. Appl. Tech. 8 (1970) 118.
[7] T. Terai, A. Suzuki, S. Tanaka, Fusion Technol. 39 (2001) 768.
[8] H. Moriyama et al., J. Nucl. Mater. 148 (1987) 211.
[9] A. Suzuki, T. Terai, S. Tanaka, J. Nucl. Mater. 258–263 (1998) 519.
[10] H. Nishimura et al., Fusion Eng. Des. 58 & 59 (2001) 667.
[11] M. Sawan, D.K. Sze, Fusion Sci. Technol. 44 (2003) 64.
[12] J.R. Keiser, J.H. DeVan, E.J. Lawrence, J. Nucl. Mater. 85 & 86 (1979) 295.
[13] M. Hara et al., Fusion Eng. Des. 81 (2006) 561.
[14] M.F. Simpson et al., Fusion Eng. Des. 81 (2006) 541.
[15] S. Fukada et al., J. Nucl. Mater. 367–370 (2007) 1190.